Splitting of charge-density and spin-density excitations of a bipolar plasma in a frequency shifter of mixed type-I and type-II quantum wells

B. Fluegel, L. N. Pfeiffer, K. West, and A. Mascarenhas

Phys. Rev. B **97**, 235313 — Published 28 June 2018

DOI: 10.1103/PhysRevB.97.235313

Splitting of charge-density and spin-density excitations of a bipolar plasma in a frequency shifter of mixed type-I and type-II quantum wells

B. Fluegel,[1] L. N. Pfeiffer,[2] K. West,[2] and A. Mascarenhas[1]

1 *National Renewable Energy Laboratory, 15013 Denver West Blvd., Golden, CO 80401, USA.*

2 *Department of Electrical Engineering, Princeton University, Princeton, NJ 08544, USA.*

The Raman frequency of the intersubband charge-density excitation plasmon in type-I type-II quantum wells is known to be very sensitively controlled via a low-power optical pump signal. We find that above a threshold electron density of approximately $4 \pm 2 \times 10^{10}$ cm^{-2}, the charge density plasmon mode splits first into two, and then with increasing density three closely spaced frequencies. A similar splitting occurs in the spin-density wave plasmon associated with the same intersubband transition. We analyze the results including the coupling to the longitudinal optical phonon and hypothesize that the splittings arise from the special situation of a structure of spatially-separated bipolar plasmons.

I. Introduction

Inelastic light scattering in modulation doped single (SQW) and multiple (MQW) quantum wells has allowed extensive measurement of the collective modes of motion in two dimensional electron gases (2DEG). The spectrum and dispersion of these modes are strongly dependent on the 2DEG density, thus motivating schemes of various complexity to vary this density within a single device. In undoped structures, densities of somewhat hot electrons were varied simply by photogenerating carriers under very high laser intensity.[1] Doped electron densities can be varied over a wide range by applying a vertical electric field across the QW, thus driving the asymmetrically doped electrons out of the well.[2] This has the undesired effect that the bands bent by the space-charge field are simultaneously "unbent", changing their confined electron levels and complicating analysis. Periodically doped *nipi* homostructures[3] allow high variable densities to be generated optically, but their bandstructure is significantly modified and it further changes under optical excitation.

An ideal device that exhibits the necessary controllable density is the mixed type I - type II quantum well[4] (MTQW) which is type I (spatially direct transitions) in absorption while being type II (spatially indirect) in emission. The MTQW is a highly effective charge separation device that can achieve high carrier densities under weak continuous wave illumination. It consists of a narrow well (NW) into which light is strongly absorbed, separated from a wide well (WW) into which the photoelectrons rapidly scatter. The transfer rate is aided by a carefully designed X-band state in the barrier. The corresponding transfer of the photoholes into the WW proceeds far more slowly resulting in a charge separation between holes in the NW and electrons in the WW. This charge separation impedes recombination[5] resulting in high WW electron density and NW hole density.

Based on the energy shift of the scattered laser light and the dependence of that shift on optically-excited electron density, the MTQW was proposed and demonstrated as an all-optical frequency shifter.[6] It used a microwatt control beam exciting the NW to change the frequency of the outgoing signal light over a linear range near 9 THz. This was the device's most sensitive range, and the light scattering mechanism is understood to be the upper branch of the coupled mode that arises from longitudinal optical (LO) phonon and the intersubband charge density excitation plasmon[7] (CDE) of the WW. However, the limitations to that frequency range were not fully investigated. Our results below using higher electron density and polarization analysis shows that the shifting coupled plasmon-phonon mode splits above a critical density and is further modified by coupling with the barrier phonon.

II. Experiment

Our MTQW frequency shifter consists of five periods of: a 26 Å GaAs narrow well, 102 Å AlAs barrier, 198 GaAs wide well, and a second barrier. The WW, which will host the 2DEG studied here, has its lowest confined optical transitions at 1.522 eV at low temperature; for the NW it is

1.92 eV (Ref. 8). As shown below, there is a large difference, by a factor of over 300, in the efficiency of WW electron generation indirectly excited by laser excitation above the NW absorption edge compared to excitation below it, i.e., directly in the WW. Raman measurements are therefore done using a two-beam measurement in which the electron population is controlled at the microwatt level using a 2.3 eV excitation laser above the NW energy. This electron population will be unaffected by the mW power of the second laser which measures the Raman scattering at an energy below the NW absorption. The Raman laser at 1.857 eV is also resonant with the GaAs spin-orbit bandedge. Excitation and collection were arranged in a backscattering geometry with a variable angle between the sample normal and the lasers. The scattering was analyzed both parallel and orthogonal to the incident laser polarization. All measurements were done at 10 K. The sample was previously measured using photoluminescence lineshape analysis to determine the electron concentration as a function of excitation intensity.[8] All of the light scattering results shown below were qualitatively reproduced in a second sample[9] grown in a different laboratory using the identical WW-NW-barrier design.

III. Results and Discussion

In the NW, the quantized levels of both the electron and hole are widely separated and their intersubband spacings are thus outside the measurements' spectral region. In the WW, the lowest two confined electron levels at low density are calculated to be 12 and 48 meV, leaving the intersubband spacing E_{01} very close to the LO phonon energy E_{LO}. The space charge due to photogenerated excitation of electrons in the WW and holes in the NW gives a symmetrical band bending[10] that will have a smaller effect on E_{01} compared to the asymmetrical potential generated by one-sided modulation doping.[11] With E_{01} close to E_{LO}, we expect strong coupling between the LO phonon and CDE. Without knowing the ordering of the two closely-separated uncoupled energies, we expect the lower quasi particle to drop asymptotically toward E_{TO} as E_{01} increases with electron density, and the upper quasiparticle to similarly rise toward E_{01}.

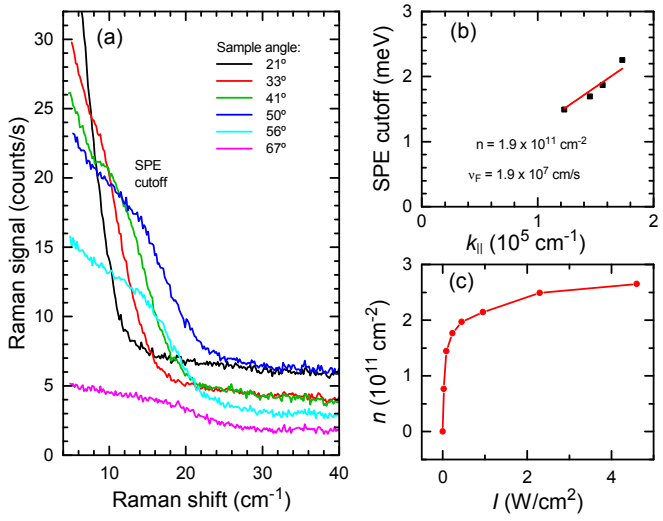

FIG. 1. Single particle excitations. (a) Spectra in the orthogonal polarization exhibiting a cut off on the high energy side. (b) Fit of the cutoff to $\hbar k_{\parallel} v_F$ yielding the Fermi velocity and electron density. (c) Scaled data from Ref. 8 calibrating the electron density to excitation laser intensity.

We first characterize in Figure 1(a) the wavevector dependence of the low-frequency intrasubband light scattering in the orthogonal polarization. The peak extending from 0 cm^{-1} at larger sample

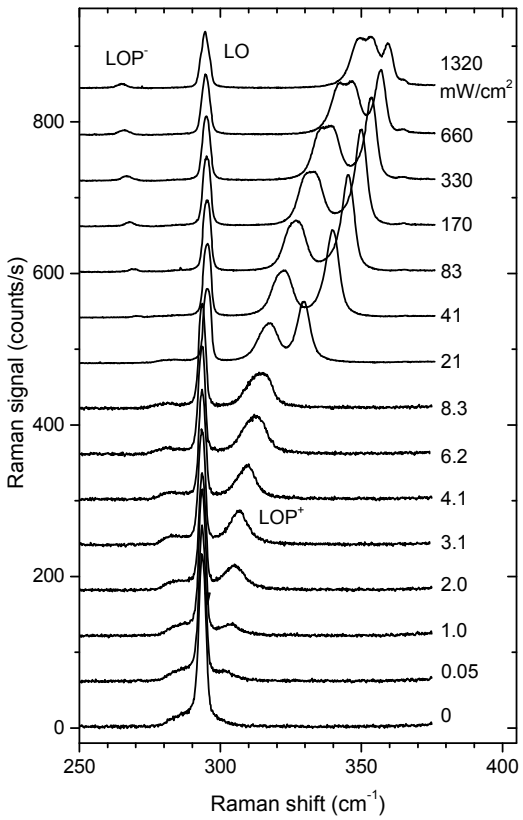

FIG. 2. Light-scattering spectra taken in the parallel polarization configuration under different values of the excitation beam intensity. Curves are displaced vertically and the intensity values are shown to the right.

angles is the spin-flip single particle continuum[12]. As the sample angle is increased, the distinct shoulder seen on the high-energy side of this peak marks the upper edge of the single particle excitation (SPE) continuum determined by $\hbar k_{\|} v_F$ where $k_{\|}$ is the wavevector parallel to the layer and v_F is the Fermi velocity.[12] The fit for several larger values of the SPE cutoff energy and $k_{\|}$ are shown in Fig. 1(b) yielding a density of $n = 1.9 \times 10^{11}$ cm^{-2} under a continuous wave excitation of only $I = 0.33$ W/cm^2. This density is within a factor of 2 from that obtained by the nonlinear function $n_e(I)$ measured by a PL lineshape analysis on the same sample in Ref. 8. For our results we use the function of Ref. 8 scaled to agree with Fig. 1(b). This relation is shown in Fig. 1(c). The maximum Fermi energy reached for the electron population in the following work will be 8 meV corresponding to $n_e = 2.2\times10^{11}$ cm^{-2}, occupying only the lowest subband.

In Fig. 2, $k_{\|}$is set to 0 and all intrasubband transitions are thus absent from light scattering. The intersubband transitions are seen in the higher energy range around E_{01}. Light scattering spectra measured in the parallel polarization are plotted for different values of the excitation laser intensity. With increasing power, the plasmons shift in frequency reflecting the increased electron density, n_e. Electron generation by the Raman laser, which is below the NW absorption edge, is far less efficient. For example the Raman laser intensity needed to replicate the plasmon energies in the spectrum labeled 2.0 mW/cm^2 is greater than this by a factor of 8000 in the absence of the excitation laser.

Below approximately 10 mW/cm^2 the plasmon spectrum consists of results similar to those reported in Ref. 6: the coupled[13] CDE plasmon - LO phonon modes, LOP$^+$ and LOP$^-$ respectively increasing and decreasing in energy with increasing excitation power. Above this power, LOP$^+$ splits into two peaks. A closer examination of the two peaks' energies, linewidths and amplitudes near this splitting on a similar sample (not shown), identifies the lower-frequency peak as the one which evolves continuously from the single low-power peak. With further increase in density both LOP$^+$ peaks increase in energy and at 170 mW/cm^2 a third peak splits off on the low energy side. The LOP$^-$ begins at low density as a broad shoulder on the LO phonon, decreasing in energy as the density increases.

These results are summarized in Fig. 3 where the frequencies of the plasmon peaks seen in Fig. 2 are plotted as a function of n_e. The high-power light scattering curve replotted in Fig. 3(a) identifies the symbols used for each peak in Fig. 3(c). There, the split upper branches labeled LOP^+ and the lower branch labeled LOP^- agree with the solid lines which are the calculated results of coupled LO-phonon-plasmon modes when the intersubband spacing E_{01} is very close to E_{LO}. We have assumed without loss of generality that E_{01} is slightly larger. As predicted by the coupling,[13] increasing photogenerated electron density results in the CDE and LOP^+ energies increasing from E_{01} whereas the LOP^- energy decreases to the energy of the TO phonon. The LOP solid curves were fit to the measured points using a value for the Coulomb interaction matrix element of 1.5 nm which agrees well with the value found in Ref. 7 for 204 Å wells. The calculations in Fig. 3(c) do not include a contribution from band bending. In single-sided modulation-doped Type I QWs that are commonly used for light scattering measurements, self-consistent calculations of subband energies[11] show a widening of E_{01} with increasing doping. The present MTQW is also a space-charge structure, however the charge is symmetrically spaced around the well, resulting in less change to E_{01}. Modeling a possible band bending as a phenomenological linear increase to the CDE energy pushes both of the LOP branches to higher energy in disagreement with the measured data points. We therefore conclude that the effect of band bending on the CDE energy is small compared to the increase via the Coulomb interaction.

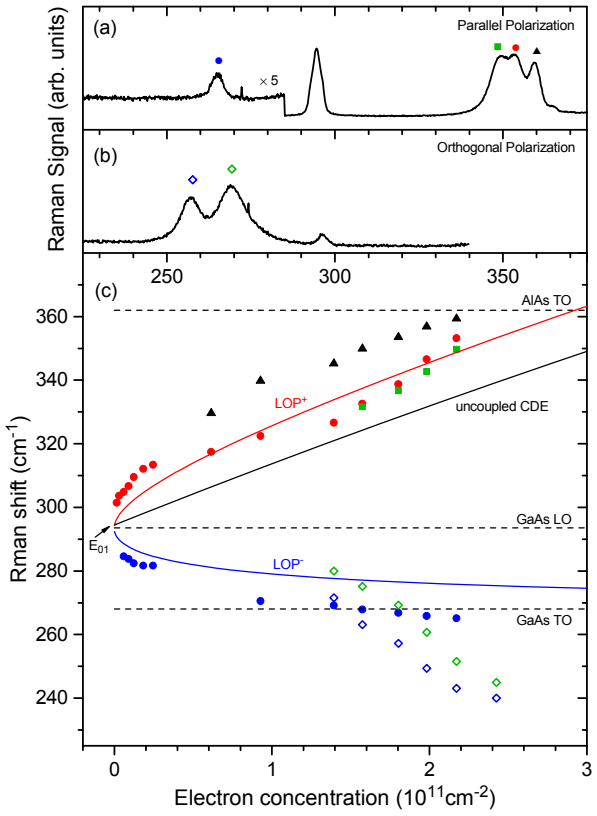

Fig. 3. Energies and fittings of plasmon peaks measured in parallel polarization (solid symbols) and orthogonal polarization (open symbols). (a) parallel polarization light scattering spectrum at 1320 mW/cm^2 showing the LOP^- and three LOP^+ peaks. (b) orthogonal polarization spectrum at 330 mW/cm^2 showing the two SDE peaks. (c) Energies of plasmon peaks (symbols identified in (a) and (b)) as a function of electron density using the calibration of Fig. 1(c). Solid curves are solutions of the coupled plasmon-LO phonon mode energies and the density-dependent CDE energy.

In the orthogonally polarized light scattering, a split peak is seen below the LO phonon energy. Fig. 3(b) shows one such spectrum whose peak energies are extracted and displayed as open symbols on Fig. 3(c). The split peak is identified as the spin-density excitation (SDE) plasmon based on the polarization and density dependence. The latter agrees with the expected

behavior of an SDE,[14] i.e., the energy drops with increasing n_e from its low-density value of E_{01} and is unaffected by the phonon crossing.

The origin of the splitting at elevated density in both LOP^+ and the SDE is unknown. One possibility is that unequal electron populations are being photogenerated among the 5 repetitions of the WW due to linear attenuation of the excitation laser. However, this is inconsistent with the LOP^+ splitting being absent at low power. As seen in Fig. 1(c), the electron population is most sensitive upon laser power in the low-power region and the LOP^+ energy's increase with density is also strongest in this density region (Fig. 3(c)). The lack of splitting in LOP^- (Fig. 3(a)) further argues against a non-uniform electron population. Another possibility was suggested in Ref 15 where a 6-meV splitting of the CDE associated with the excited state electron transition $E_0 \rightarrow E_2$ (but not its SDE) was attributed to a close match of this energy with E_{LO}. This may refer simply to the LOP^+ - LOP^- splitting, which is not the present situation. In either case, our MTQW LOP^+ splits only after its energy has moved well above E_{LO} and where n_e is above a threshold density that is in the range $2 - 6 \times 10^{10}$ cm^{-2}. That electron density is well exceeded in previous studies of modulation doped wells,[12,7,14] however a unique aspect of the MTQW is the bipolar plasma that is generated with electrons in the WW and holes in the NW. Theoretical works[16, 17] have shown that coupling between spatially separated bilayers, either bipolar or unipolar, results in a new coupled mode, an undamped acoustic mode. Experimentally this has been demonstrated for the case of an electron bilayer,[18] but those results concern only the low-frequency intraband spectral region. There has been no prior work on a spatially separated electron-hole multilayer that would include the intersubband plasmons investigated here. This may be a fruitful direction in which to look for the physics underlying the plasmon splitting that is now observed.

The upper energy of the LOP^+ is seen in Fig. 3(c) to be bounded by the energy of the TO phonon of the pure AlAs barrier. This phonon can be seen in the shoulder at approximately 365 cm^{-1} in Fig. 3(a) and its energy is plotted in Fig. 3(c). Further increase in the excitation power beyond that shown caused the three LOP^+ peaks to converge without exceeding the AlAs TO energy. This clamping effect below the phonon energy would be well understood in the case of a phonon in the *quantum well layer* as it couples with the rising plasmon, however, Fig 3 suggests that a similar coupling exists between the plasmon in the well and the ionic oscillation in the barrier. This is analogous to other cases of coupling between spatially separated excitations such as surface plasmon polaritons or coupled plasmons in bilayers.[16]

In conclusion, the physical mechanisms governing light scattering in the MTQW at low electron densities do not hold for densities beyond 4×10^{10} cm^{-2}. In addition to a coupling with the barrier phonon, the light shifted beyond this limit is split by interactions that require further theoretical study.

IV. ACKNOWLEDGMENTS

This work was authored in part by Alliance for Sustainable Energy, LLC, the manager and operator of the National Renewable Energy Laboratory for the U.S. Department of Energy (DOE) under Contract No. DE-AC36-08GO28308. Funding provided by U.S. Department of Energy, Basic Energy Science, Division of Material Sciences. The views expressed in the article do not necessarily represent the views of the DOE or the U.S. Government. The U.S. Government retains and the publisher, by accepting the article for publication, acknowledges that the U.S. Government retains a nonexclusive, paid-up, irrevocable, worldwide license to publish or reproduce the published form of this work, or allow others to do so, for U.S. Government purposes.

1. A. Pinczuk, J. Shah, A. C. Gossard, and W. Wiegmann, Phys. Rev. Lett. **46**, 1341 (1981).
2. A. R. Goñi, U. Haboeck, C. Thomsen, K. Eberl, F. A. Reboredo, C. R. Proetto, and F. Guinea, Phys. Rev. B **65**, 121313(R) (2002).
3. Ch. Zeller, B. Vinter, G. Abstreiter, and K. Ploog, Phys. Rev. B **26**, 2124 (1982).
4. P. Dawson, I. Galbraith, A. I. Kucharska, and C. T. Foxon, Appl. Phys. Lett. **58**, 2889 (1991).
5. P. Dawson and M. J. Godfrey, Phys. Rev. B **68**, 115326 (2003).
6. B. Fluegel, A. Mascarenhas, D. W. Snoke, L. N. Pfeiffer, and K. West, Nat. Photonics **1**, 701 (2007).
7. A. Pinczuk, J. M. Worlock, H. L. Störmer, R. Dingle, W. Wiegmann, and A. C. Gossard, Solid State Commun. **36**, 43 (1980).
8. R. Guliamov, E. Lifshitz, E. Cohen, A. Ron, and L. N. Pfeiffer, Phys. Rev B **64,** 035314 (2001).
9. A. Mialitsin, S. Schmult, I. Solov'yov, B. Fluegel, and A. Mascarenhas, Superlattices and Microstructures **51**, 834 (2012).
10. G. Bastard, *Wave Mechanics Applied to Semiconductor Heterostructures* (Les Editions de Physique, 1990) ch. V.
11. C. Schüller, *Inelastic Light Scattering of Semiconductor Nanostructures* (Springer, Berlin Heidleberg, 2006).
12. G. Fasol, N. Mestres, M. Dobers, A. Fischer, and K. Ploog, Phys. Rev. B **36**, 1565 (1987).
13. A. Pinczuk and G. Abstreiter in *Light Scattering in Solids V Superlattices and Other Microstructures*, edited by M. Cardona and G. Güntherodt (Springer-Verlag, Berlin Heidleberg, 1989).
14. A. Pinczuk, S. Schmitt-Rink, G. Danan, J. P. Valladares, L. N. Pfeiffer, and K. W. West, Phys. Rev. Lett. **63**, 1633 (1989).
15. A. Pinczuk and G. Abstreiter in *Light Scattering in Solids V Superlattices and Other Microstructures*, edited by M. Cardona and G. Güntherodt (Springer-Verlag, Berlin Heidleberg, 1989), p.177.
16. S. Das Sarma and A. Madhukar, Phys. Rev. B **23**, 805 (1981).
17. G. E. Santoro and G. F. Giuliani, Phys. Rev. B. **37**, 937 (1988).
18. D. S. Kainth, D. Richards, A. S. Bhatti, H. P. Hughes, M. Y. Simmons, E. H.Linfield, and D. A. Ritchie, Phys. Rev. B **59**, 2095 (1999).